SLAC – PUB – 4553
March 1988
(I/E)

# A SILICON VERTEX DETECTOR FOR A B FACTORY*

VERA LÜTH

*Stanford Linear Accelerator Center*
*Stanford University, Stanford, California,* **94309**

## ABSTRACT

The design of a Silicon vertex detector for a high luminosity $e^+e^-$ linear collider is discussed, with emphasis on the choice of parameters for the layout, resolution and segmentation.

## 1. Introduction

In recent years, experiments at $e^+e^-$ storage rings PEP, PETRA, DORIS, and CESR have demonstrated that vertex detectors with moderate resolution ( 50 – 100 $\mu$m ) mounted on the outside of a thin walled vacuum pipe can substantially enhance the sensitivity in the detection of the decays of heavy leptons and heavy flavour hadrons. A vertex detector with much improved resolution will provide a high precision point and angle measurement for charged tracks close to the beam-beam interaction point, and will thereby complement the momentum measurement in the main tracking chamber. At a high luminosity storage ring designed to operate at the $\Upsilon(4s)$ and above, such a system will allow for

— the measurements of multiple vertices in events and permit the separation of charm and beauty decays from light quark background events;

— a substantial reduction in the combinatorial background in B and D decays;

— a substantial reduction in the hadronic and Bhabha background in $\tau$ decays;

— the measurement of lifetimes of heavy flavour or any other particles with decay times exceeding $10^{-13}$ s;

— the study of decay time dependent effects in $B\overline{B}$ and $D\overline{D}$ states, and

— an enhanced sensitivity in the detection of the Higgs or other new particles.

*Contribution to the Workshop on a High Intensity $e^+e^-$ Linear Collider.*
*Courmayeur, Italy, December 14-18, 1987*

* Work supported by the US Department of Energy, contract DE-AC03-76SF00515 and by the Laboratori Nazionali di Frascati dell'INFN.

## 2. Design Parameters

The principle task of a high precision vertex detector at a B factory is clearly the measurements and separation of decay vertices of charm and beauty particles. Table I lists the average decay distances for B decays at the $\Upsilon(4s)$ for different colliding beam configurations, i.e. for a machine which produces the $\Upsilon(4s)$ at rest ($\beta = 0$) and for machines which produce the $\Upsilon(4s)$ resonance with a velocity $\beta$ relative to the laboratory frame. In $\Upsilon(4s)$ decay, the $B\overline{B}$ pair is produced just above threshold. There are no additional particles that originate from the beam-beam interaction point. In most applications, the relevant distance is not the decay length of a single B, but the distance between the decay points of the two B mesons and therefore the knowledge of the interaction point is not as important as in previous experiments. In most $B\overline{B}$ events, we expect a total of four vertices, one from each B decay, and one from each D decay. The required vertex resolution should clearly exceed the average B decay length by a factor of five or more. For a symmetric machine which produces the $\Upsilon(4s)$ at rest, this places demands on the vertex detector precision that will be extremely difficult to meet. Nevertheless, even if the decay time distributions cannot be measured with high accuracy, a vertex detector with a of $20-30$ $\mu$m will substantially improve the B reconstruction by separating B and D decay vertices. For an asymmetric machine the boost direction coincides with the direction of the higher energy beam, and consequently the increase in the decay length is to be found only in this direction. Decay lengths in the plane transverse to the beams remain unchanged, of course. In general, the vertex measurement alone will not be sufficient to disentangle the tracks in a given event, but this information needs to be combined with the kinematics and the particle identification for all tracks involved, charged and neutral. However, there are some very clean event topologies that are easy to identify. Decays of the kind $B \rightarrow \psi + anything$ have the advantage that the $\psi$ decay marks the B decay point. Leptonic decays $\psi \rightarrow e^+e^-, \mu^+\mu^-$ give a striking signature of two leptons with high transverse momentum. Detailed Monte Carlo studies will be necessary to evaluate the physics advantage of an asymmetric $\Upsilon(4s)$ collider versus the difficulties in particle detection in a system that is boosted strongly towards the direction of the higher energy beam.

Table I: Decay distances for beauty and charm decays at the $\Upsilon(4s)$ resonance in a c.m. system moving with velocity $\beta$.

| Distances ($\mu$m) | $\beta$=0.0 | $\beta$=0.4 | $\beta$=0.7 |
|---|---|---|---|
| $B$ decay | 28 | 169 | 355 |
| $D$ decay | 98 | 265 | 530 |
| $B - \overline{B}$ | 58 | 180 | 370 |
| $D - \overline{D}$ | 170 | 270 | 470 |
| $B - D$ | 85 | 115 | 185 |

A further difficulty in detecting B vertices at $\Upsilon(4s)$ arises from relatively low momenta of most the secondary particles. In Figure 1 the spectra for a specific semi-leptonic B decay are shown.[1] Even in a boosted system with $\beta = 0.7$, most of the particle momenta remain small.

In practice, vertices are obtained from a fit of several tracks extrapolated from the measured position in the detectors to a common point of origin. The error on the extrapolation of a track from the detectors to the decay point can be written as the sum of four major terms,

$$\sigma^2 = a^2 + (b/p)^2 + c^2 + d^2,$$

where the first term represents the extrapolation error due to the layout of the vertex detector, its intrinsic resolution, the number of detector planes and their distances relative to the beam. The second term gives the contribution caused by multiple scattering of the particle in the material up to the first detector,

$$b = \sum_k R_k \, \Delta\Theta_k.$$

Here

$$\Delta\Theta_k = 0.014 \cdot \sqrt{\frac{\Delta X_k}{X_0}}$$

is the width of the distribution of scattering angles for a particles of momentum $p = 1 \; GeV/c$ passing through material of thickness $\Delta X_k/X_0$ located at a distance $R_k$. The third term accounts for the degradation in the position resolution in a silicon detector for non-normal incidence. The fourth term d accounts for additional contributions to the error on the impact parameter that are not included in the first three terms. These are, for example, errors in the placement of the detectors, instabilities in their position with time and possible temperature effects. Also instabilities in the position of the beam-beam interaction point would be included in this term. But remember, for B decay time measurements, knowledge of the interaction point is not absolutely required.

The first term is most strongly controlled by the design of the vertex detector. As a simple example, let us study a detector that consists of only two layers, placed at distances $R_i$ and $R_o$ from the interaction point. The intrinsic space resolution for the two layers be denoted by $\sigma_i$ and $\sigma_o$. Then the error on the track extrapolated to the interaction point is

$$a^2 = \left(\frac{R_i \, \sigma_o}{R_o - R_i}\right)^2 + \left(\frac{R_o \, \sigma_i}{R_o - R_i}\right)^2.$$

Figure 2 shows the dependence of the total impact parameter error on the distances $R_i$ and $R_o$, and the intrinsic detector resolution. The curves presented in these

graphs take into account the multiple scattering in a 300 $\mu$m thick Beryllium beam pipe, lined with 4 $\mu$m of Titanium. The detector thickness is taken to be 200 $\mu$m. All these curves assume normal incidence, i.e. the track length is equal to the distance between the layers. It is obvious from these curves and the simple relations spelled out above that the resolution and radial position of the closest detector layer are the most important parameter. The distance between the two detector layers determines the angular resolution of the vertex detector. For 40 mm spacing, one obtains typically 0.3 mrad, given a 0.005mm point resolution. The influence of the multiple scattering in the beam pipe and the detectors on the total error is illustrated in Figures 3 for detector distances $R_i = 10\ mm$, $R_o = 40\ mm$ and resolution $\sigma_i = 0.005\ mm$. For momenta below 1 GeV/c, the influence of the multiple scattering becomes dominant. This momentum dependence is shown in Figure 4.

Consequently, one can derive the following design rules for a vertex detector made of individual layers:

— The resolution of the innermost layer should be as good as possible.

— The innermost layer should be placed as close as possible to the interaction point.

— The amount of material in beam pipe and the thickness of the detectors should be minimized.

The performance limits are not set by the intrinsic resolution of the silicon devices, but by the multiple scattering in the material of the vacuum pipe and the detector support structure. The most important parameter is the distance of the first detector from the beam and this will be determined by the machine characteristics and the collimation and shielding to protect against the radiation background.

## 3. Solid State Vertex Detectors

Silicon detectors with finely segmented electrodes are an outgrowth of the semiconductor counters that have been used in nuclear physics for more than twenty years. In high energy physics, their use as high resolution tracking devices was pioneered by two groups CERN[2,3] Since then, many other experimenters have built on this experience and have employed commercially available Silicon detectors with strip and pixel read-out in fixed target experiments. At present, the construction of several silicon vertex detectors is underway for $e^+e^-$ experiments at LEP and PEP. These projects are the first to face the constraints and challenges that a colliding beam experiment introduces into the art of building such devices. Any future detector of this kind will greatly benefit from the experience to be gained in their construction and operation.

Silicon strip detector vary greatly in their dimensions, some have up to thousand strips. The minimum pitch realised so far is 12.5 $\mu$m, the maximum length

is 90mm, limited by the 4" diameter of the silicon wafer. Various read-out methods have been used, depending on the spatial resolution and two-track separation required. Most experiments have used analog pulseheight information and determine the exact position of the particle trajectory by a pulseheight weighted mean of the strip coordinates. The best resolution achieved so far is 2.5$\mu$m. To reduce the number of read-out channels, several experiments have used capacitive coupling between the strips with acceptably small degradation in resolution.

The advantages of silicon detectors are the following:

— good localisation of the ionisation charges due to short range of electrons and photon in the material, limited diffusion of the drifting charges;

— large ionisation statistics due to the narrow band gap and low ionisation potential, 80 e-hole pairs per $\mu$m;

— good mechanical rigidity allowing for low mass support structures;

— VLSI technology guaranteeing high precision in the fabrication of the strip diodes, and a potential of full integration of detector elements with the circuitry necessary for amplification and read-out.

The main drawback of finely segmented arrays of Silicon micro-strip detectors have been so far

— the large volume and cost of the read-out electronics,

— the long time required for sequential read-out,

— the thickness of the detectors, typically 300 $\mu$m,

— the one-dimensional read-out, and

— the sensitivity of VLSI electronics and CCDs to radiation damage.

Concerted efforts are presently underway to overcome most of these deficiencies. Several groups have been developing custom designed VLSI circuits that contain the electronics for a large number of channels on a few mm$^2$. The problem of existing designs are the rather large power dissipation and the sensitivity of these circuits to exposure to ionizing radiation. Tests of NMOS and CMOS circuits are presently underway at SLAC, Rutherford Laboratory, and Munich.[4–6] The thickness of the detectors determines the amount of charge produced by ionisation, for a thickness of 300 $\mu$m and a strip pitch of 25 $\mu$m and length of 8 cm, typical signal to noise ratios of 20:1 have been obtained for minimum ionising particles at normal incidence. Given the expected improvements in electronics, strips or pixels of smaller capacitance, and possibly a reduction in the operating temperature, substantially thinner detector will be feasible in the near future. Thinner depletion depths will also prevent the degradation of the resolution for tracks of non-normal incidence, which is caused by the spread of the ionisation charges over many of the narrow read-out strips. The thinner detectors will reduce the multiple scattering, but will also reduce the mechanical strength of the detectors which may result in the need for external support. At CERN, detectors with double-sided read-out are

under study for installation at LEP. Such a read-out is achieved by segmenting the back-plane of the detector, in addition to the strips on the top. This will result in more than one coordinate per detector, but will not necessarily eliminate coordinate ambiguities due to multiple hits per detector.

Alternatives to the concept of strip read-out are pixel devices with truly two-dimensional coordinate read-out. Charged Coupled Devices (CCD) which store the ionisation in two-dimensional potential wells are commercially available and have been used successfully in a fixed target experiment at CERN. Typical pixel sizes are 22 $\mu$m x 22 $\mu$m in arrays of several cm$^2$. The shallow depletion depth of CCDs is only 12 $\mu$m resulting in about 1000 charge carriers per minimum ionising particle, this makes cooling of these devices mandatory. New concepts for pixel devices with fast selective readout are being developed in preparation for experiment at the SSC. On the other hand, this shallow depth prevents a degradation of performance for non-normal incidence which is observed for the much thicker strip detectors. The disadvantage of the CCDs is the rather long read-out time. Developments are under way to increase the speed by orders of magnitude to 300 Mhz.[7,8] Another very challenging development that aims at full two-dimensional read-out are Silicon drift chambers, in which the internal field in the Silicon forces the charge to drift parallel to the plane with drift time measurements to locate the signal along the strip.[9] Preliminary tests have produced very encouraging results.

## 4. Lay-out of a Vertex Detector

The general lay-out of a silicon vertex detector is given in Figure 5. We have assumed that over a length of 30 cm or so the beam stay clear area is such that active detector elements can be placed as close as 10 mm from the beam center. We have chosen to place the detector outside of the vacuum chamber because this will avoid problems of assembly, access and vacuum feedthroughs and will not increase the amount of multiple scattering so critical here. If we accept beryllium as the strongest material per radiation length then the required thickness of about 0.3mm ($8.3\ 10^{-4} X_0$) is a good match to the skin depth needed to shield detectors and low noise electronics from the e.m. radiation of the beam. In practice, it is probably advisable to add a lining of a few $\mu$m of titanium on the inside, to absorb soft photons from synchrotron radiation.

The detector is layed out to be cylindrically symmetric relative to the beam direction. All elements can be supported from the outer radius allowing for the beam pipe to move independently. The detector is divided into a central and two identical forward sections. The total solid angle coverage is 0.99 of $4\pi$, the central section extends to $cos\theta$=0.7. The central section is divided into two inner and two outer layers. In principle, one only needs one layer each. In practice, there are detection losses due to dead channels, support structures and edges, and possibly inefficiencies in thinly depleted devices, so that the addition of another layer reduces the detection losses. The modules are arranged in polygons of six and twelve sides

such that the innermost layer of each pair has almost complete coverage, while the outer layer has gaps at the corners. Also, there is room for read-out on two sides of the rectangular detector elements. There are many choices for segmentation of the detectors, and the choice will depend on the technology available in a few years time. For the inner two layers of the central section, pixel read-out is preferred, because it avoids ambiguities in the reconstruction of tracks and provides good resolution in two dimensions. On the other hand, for a subdivision of each module into three individual detectors, there will be 36 detectors per layer compared to an average of 12 charged particles per event, so that the ambiguity in the coordinate assignment is not expected to be a very severe problem. For the outer two layer of the central section, double sided strip read-out will be adequate.

The forward detectors consist of two pairs of circular discs with double sided strip read-out. One attractive way of laying out strips on a circular surface is to use *logarithmic spirals*, with opposite curvature on the two sides of the detector. The layout of the strips is given in Figure 6. This arrangement of strips provides uniform segmentation in the azimuth ($\phi$) and in the polar acceptance ($cos\theta$) over the full surface. All strips end on the inner and outer periphery of the disc thus allowing for easy connections. The radial coordinate is simply obtained from the difference in the strip numbers, the sum of the strip numbers specifies the azimuth $\phi$ of the hit.

## 5. Segmentation

The segmentation of the detector affects its resolution in two ways: it determines a) the two-track resolution and b) the point resolution. Given that there are on the average 12 charged particles produced more or less isotropically at the $\Upsilon(4s)$ the requirements on the granularity of the detector are not at all a factor in the design. The point resolution is, however, next to the radius of the innermost layer, the most important parameter to chose. If we assume that the vertex position will be determined by the highest momentum particle that cross at large angles then it might be an advantage to get the best possible point resolution, even though most of the other tracks undergo substantial multiple scattering. We therefore choose the best resolution that is feasible, namely $\sigma_i$=0.005mm, in the $r\phi$ coordinate. This can be achieved with a strip or pixel width of 25 $\mu$m. For the outer layers and the forward section, $\sigma_o = 0.010mm$ will be adequate.

Thus, we suggest to have pixel sizes of $25\mu m \times 52.5\mu m$ for the inner two layers with 512 $\times$ 512 pixels per detector. This results in detector dimensions of 12.8mm $\times$ 26.9mm, and 3 detectors join to form a module. The expected resolution is 5 $\mu$m in the $r\phi$ direction and 10.5 $\mu$m in the z direction along the beam. In total, there will be $2 \times 3 \times 6$ pixel detectors with $2^{18}$ pixels each, giving a total of 9.4 $10^6$ pixels. Clearly, intelligent read-out schemes will need to be developed to avoid dead-time by suppressing empty channels.

The same resolution could of course be obtained with a double sided strip read-out, strips at $90^o$ with a strip widths corresponding to the dimensions quoted for the pixels. Assuming the same detector dimensions, with strips read-out on both ends and along one side, the total number of channels would be $3 \times 512$ strips per detector and 55,296 channels for two layers. The read-out along the sides can be avoided by orienting the strips parallel to the two diagonals of the detector. With the same detector dimensions, this would correspond to a stereo angle of $\alpha$=25.4$^o$. With a strip width of p=50$\mu$m, the resolution is expected to be about $r\Delta\phi = \Delta p\ sin\alpha/sin2\alpha = 5\mu$m, and $\Delta z = \Delta p\ cos\alpha/sin2\alpha = 13\mu$m along the beam direction. There would be 1024 strips per detector, and 36,864 strip for the two inner layers.

For the outer layers of the central section, diagonal strip detectors are appropriate. For a width of 24.6mm and overall length of 90 mm, the stereo angle is 14.8$^o$. There are 4096 strips of 25 $\mu$m width, resulting in 49,152 read-out channel in $2 \times 12$ detector modules in layers 3 and 4. Read-out connections are at the ends only.

For the forward disc counters with spiral read-out strips, a $\phi$ segmentation of 0.0015 radians corresponds to $2 \times 4096$ strips of identical shape per counter. The effective segmentation in $cos\theta$ is 0.00035. The resolution is typically 20% of the segmentation width.

A summary of the dimensions of the detector elements and a possible segmentation is given in Table II. If one chooses strip rather than pixels for the inner two layers of the central section, the number of elements would be substantially decreased without loss in resolution.

## 6. Resolution

The resolution of the proposed detector has been studied for a variety of layouts, segmentations, and detectors thicknesses, as a function of the particle momentum and polar angle $\theta$. Some of the results are given in Figure 7 . The angular resolution is of the order of 0.25mrad both in $\phi$ and $\theta$ for momenta exceeding 0.5 GeV/c. Detailed Monte Carlo studies of specific decay modes need to be performed to evaluate the resolution in the reconstruction of B and D decay vertices.

The curves do not include a degradation of the resolution due to non-normal incidence, denoted by the term c in our equation for the detector resolution. In a silicon detector of depletion depth t that has strips of pitch p transverse to the beam axis, the collected charge will spread over n strips, with

$$n = t/(p\ tan\theta),$$

where $\theta$ is the polar angle of the particle relative to the beam. The total ionisation increases as $s_0/sin\theta$, where $s_0$ represents the ionisation charge at normal incidence ($\theta = 90^o$). Thus for a given signal $s_0$ at normal incidence, the signal will spread

Table II: Dimensions and segmentation of the Vertex Detector.

| Parameters | Layer 1 | Layer 2 | Layer 3 | Layer 4 |
|---|---|---|---|---|
| Central Detector | | | | |
| Radius of layer (mm) | 10 | 15 | 40 | 50 |
| active length of module (mm) | 80 | 80 | 90 | 90 |
| active width of module (mm) | 12.8 | 12.8 | 25.6 | 25.6 |
| size of detectors ($mm^2$) | $12.8 \times 27$ | $12.8 \times 27$ | $25.6 \times 90$ | $25.6 \times 90$ |
| No. modules/layer | 6 | 6 | 12 | 12 |
| No. detectors/module | 3 | 3 | 1 | 1 |
| No. segments/detector | $512 \times 512$ | $512 \times 512$ | $4 \times 1024$ | $4 \times 1024$ |
| resolution in $r\phi(\mu m)$ | 5 | 5 | 5 | 5 |
| resolution in z ($\mu$m) | 10.5 | 10.5 | 13.5 | 13.5 |
| Forward Detector | | | | |
| distance from IP (mm) | 60 | 75 | 110 | 130 |
| inner radius of detector (mm) | 15 | 15 | 15 | 15 |
| outer radius of detector (mm) | 60 | 60 | 40 | 40 |
| No. segments/detector | $2 \times 4096$ | $2 \times 4096$ | $2 \times 2048$ | $2 \times 2048$ |
| resolution in $\phi$ (mrad) | 0.3 | 0.3 | 0.6 | 0.6 |
| resolution in $cos\theta$ | 0.0001 | 0.0001 | 0.0002 | 0.0002 |

over n strips with an average pulseheight per strip given by

$$\frac{s}{n} = \frac{s_0 \cdot p}{cos\theta\ (p\ tan\theta + t).}$$

The minimum is s/n $= p/t \cdot s_0$. The segmentation in the direction parallel to the beam has to be chosen such that the aspect ratio of pitch versus depletion depth is of order one, in particular, for our design we have $p/t \approx 0.5$ (p=50$\mu$m, t=100$\mu$m). For the minimum angle $tan\theta = 0.25$, the charge will spread over 400 $\mu$m, corresponding to 8 strips, the signal per channel will decrease to 0.46 $s_0$. The resolution, will depend on the overall signal to noise ratio, but for a typical ratio of 20:1, the centre of this wide charge distribution can still be measured to better than one strip width.

## 7. Mechanical Support Structure

A potential limit to the resolution of a high precision solid state vertex detector is the placement and stability of its individual elements relative to each other and to the outer tracking system. It is clearly beneficial to rigidly support the vertex detector from the surrounding tracking chamber such that their relative alignment remains unchanged over the course of a run. The relative stability of individual modules should also be maintained to the level of a $\mu$m over this period. The alignment can be monitored by tracks of high momentum charged particles traversing the detector.

Experience with the Mark II and SLD projects has shown that the time and budget required to design and build the mechanical support structure are easily underestimated. Given the miniature dimension of the device, special methods of precision fabrication and assembly have to be developed. New techniques for precision alignment need to be evaluated.

## 8. Conclusions

Based on present technology, we can design and build a silicon vertex detector that can measure impact parameters of charged particle tracks of 1 GeV/c momentum to better than 10$\mu$m over a large fraction of the solid angle. The angular resolution is of the order of 0.25 mrad in azimuth and polar angle. This can be achieved with pixel devices or double sided strip read-out of 25$\mu$m pixel or strip width provided the first active detector can be placed at a distance of 10mm or less from the beam. The design of a thin-walled vacuum chamber and the shielding of the synchrotron radiation from the final focus quadrupoles are of prime importance for such a detector. The development of low power, low noise, high density amplifiers and read-out circuits needs to be pursued so as to fit the detectors into the limited space without loss of solid angle and a substantial increase in multiple scattering. Precision assembly and alignment techniques need to be studied.

## Acknowledgements

I should like to take this opportunity to thank the INFN for the kind hospitality that was extended to me during my visit to Frascati in November 1987. I particularly owe many thanks to Ida Peruzzi and Marcello Piccolo for their efforts to make my stay such a pleasant experience.

## References


1. D. Fujino, SLAC, private communication.
2. G. Bellini *et al.*, Physics Reports **84**, 9 (1982).
3. E. Belau *et al.*, Nucl. Inst. Meth. **217**, 224 (1983).
4. J.T. Walker *et al.*, Nucl. Inst. Meth. **226**, 200 (1984).
5. P. Seller *et al.*, paper presented at the *IEEE Nucl. Science Symposium,* San Francisco (1987).
6. G. Lutz *et al.*, MPI-PAE/Exp. El. 170 (1987).
7. R. Bailey *et al.*, Nucl. Inst. Meth. **213**, 201 (1983).
8. S.R. Amendolia *et al.*, Nucl. Inst. Meth. **226**, 32 (1984).
9. E. Gatti *et al.*, Nucl. Inst. Meth. **A235** 365 (1985).


## Figure Captions

1. Examples of momentum spectra for charged particles produced in the decay $B^0 \rightarrow D^{*+}e^-\nu$, with $D^{*+} \rightarrow \pi^+K^-\pi^+$. The distributions are normalised to 1000 B decays.
2. The total error on the impact parameter measured in a detector with two planes as a function of a) the intrinsic resolution of the detector $\sigma_i$ with $\sigma_o = 2\,\sigma_i$, b) the distance between the two planes $\Delta R$ with $R_i =$ 10mm, and a) $R_i$, the distance of the first detector from the interaction point, for constant distance $\Delta R = R_o - R_i =$ 30mm and fixed resolution $\sigma_i = 0.005$mm.
3. Error on the impact parameter as a function of the thickness of a) the beryllium beam pipe and b) the silicon detectors.
4. Momentum dependence of the impact parameter for different choices of the resolution $\sigma_i$, and the radial distances $\Delta R$, and $R_i$ for a fixed resolution $\sigma_i =$ 0.005 mm.
5. Layout of a silicon vertex detector.
6. Segmentation of silicon strip detectors in the central section (a and b) and the forward section (c).
7. Resolution of the Vertex detector as a function of the polar angle $\theta$, a) impact parameter resolution and b) resolution in the azimuthal angle $\phi$.

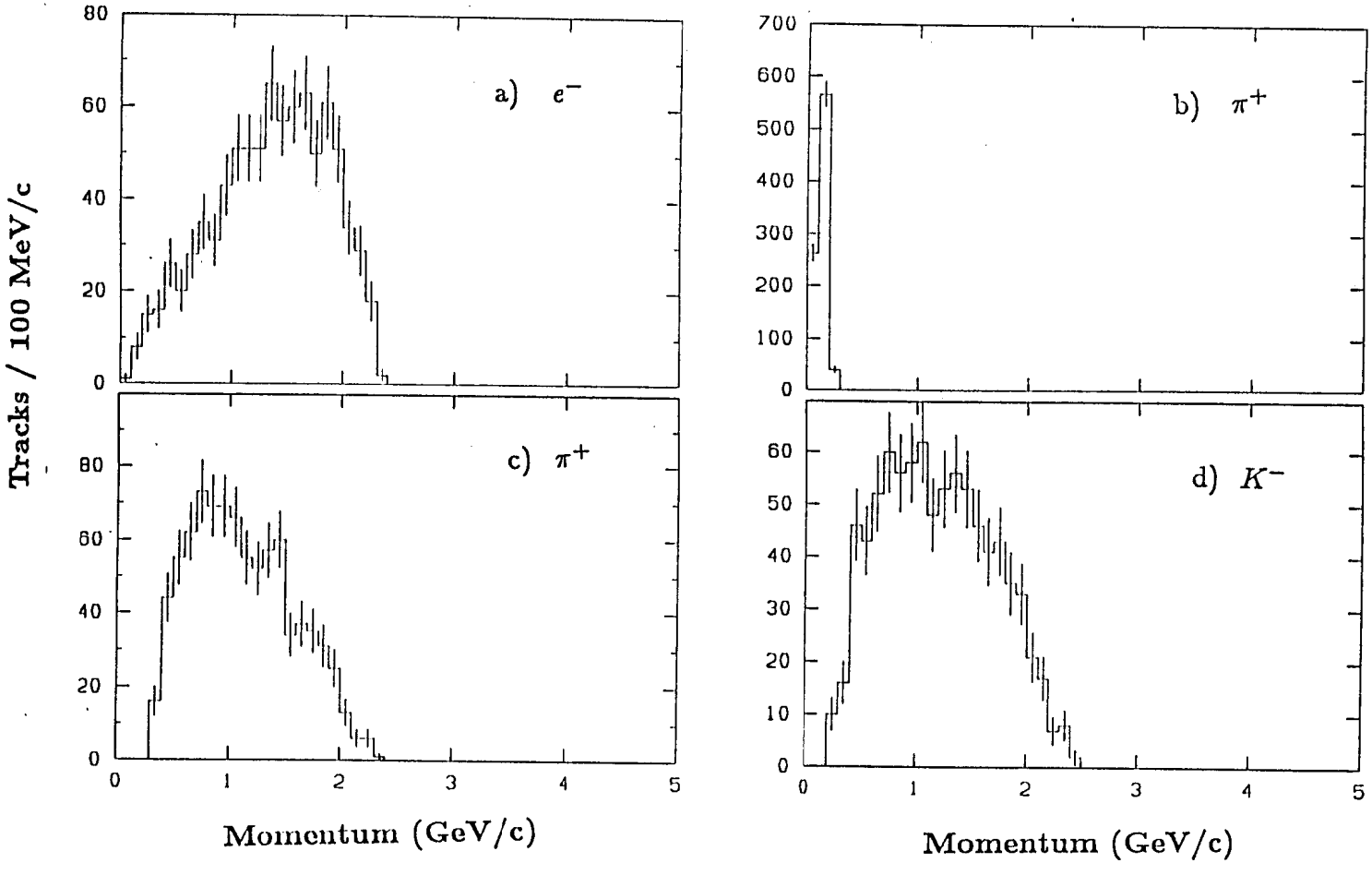


Figure 1

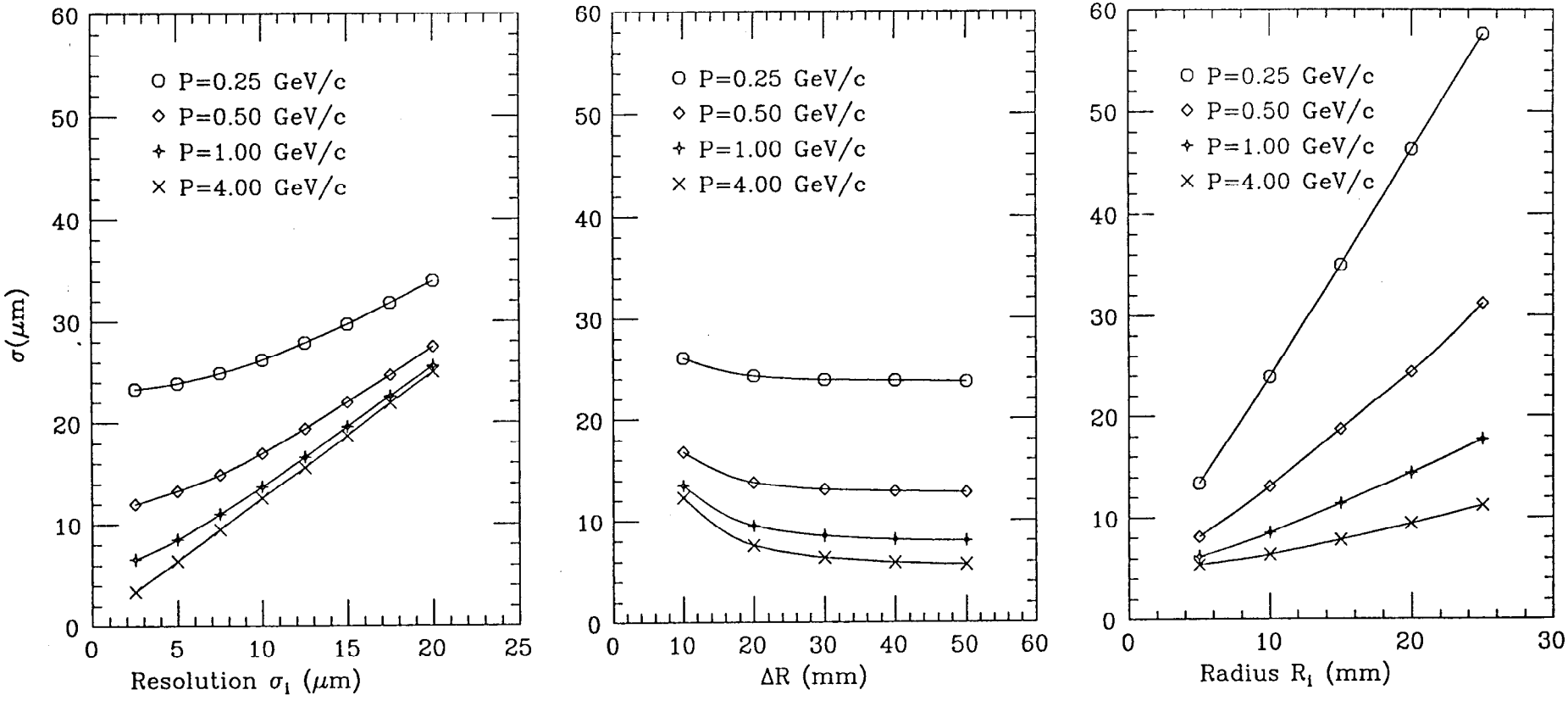
P=0.25 GeV/c
P=0.50 GeV/c
P=1.00 GeV/c
P=4.00 GeV/c
σ(μm)
Resolution σ_i (μm)
ΔR (mm)
Radius R_i (mm)

Figure 2

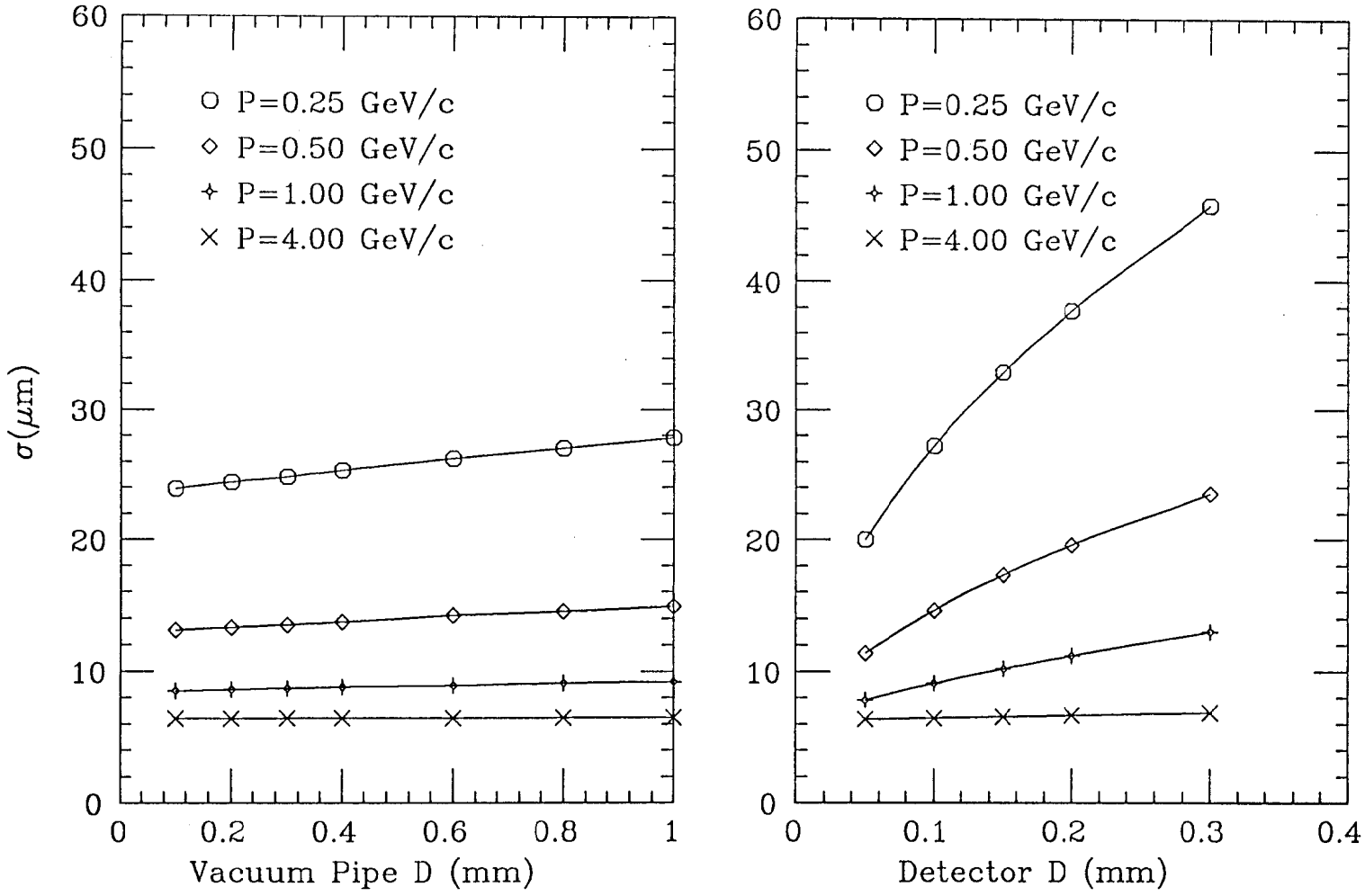
60
50
40
30
20
10
0
σ(μm)
P=0.25 GeV/c
P=0.50 GeV/c
P=1.00 GeV/c
P=4.00 GeV/c
0
0.2
0.4
0.6
0.8
1
Vacuum Pipe D (mm)
60
50
40
30
20
10
0
P=0.25 GeV/c
P=0.50 GeV/c
P=1.00 GeV/c
P=4.00 GeV/c
0
0.1
0.2
0.3
0.4
Detector D (mm)

Figure 3

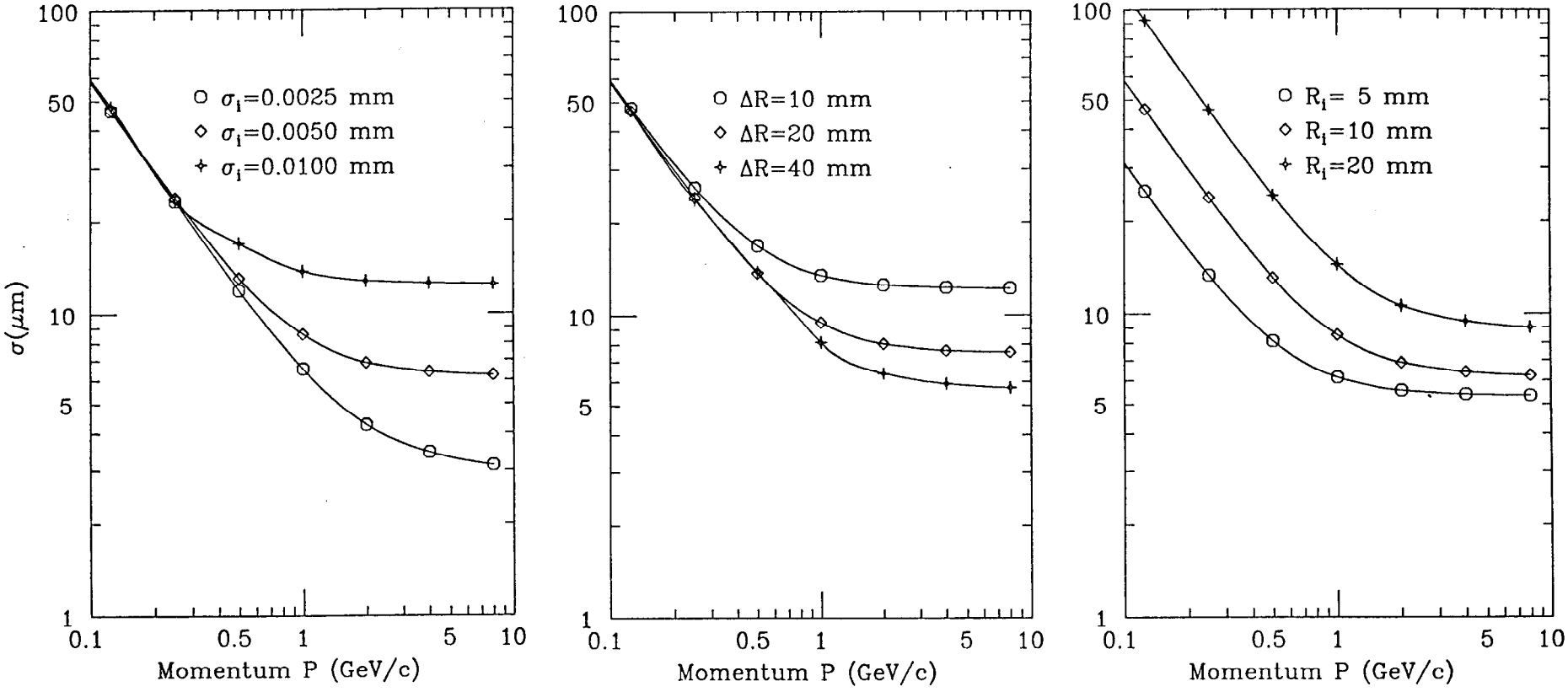
100
50
10
5
1
0.1
0.5
1
5
10
σ(μm)
Momentum P (GeV/c)
σi=0.0025 mm
σi=0.0050 mm
σi=0.0100 mm
ΔR=10 mm
ΔR=20 mm
ΔR=40 mm
Ri= 5 mm
Ri=10 mm
Ri=20 mm

Figure 4

SILICON VERTEX DETECTOR

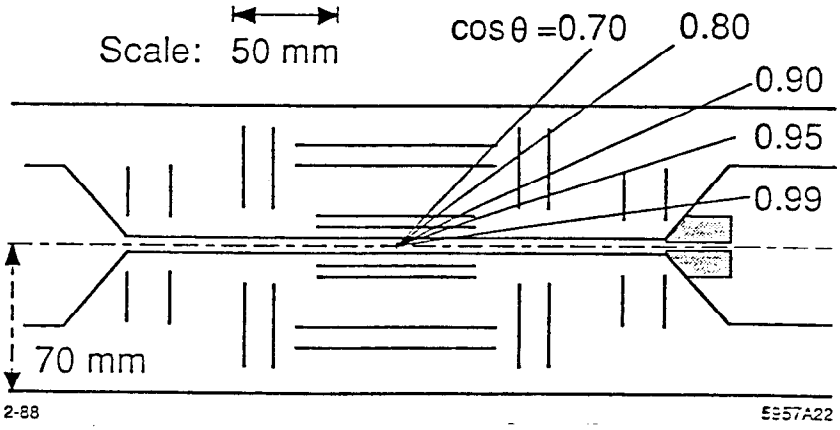


SVD ENDVIEW OF CENTRAL SECTION

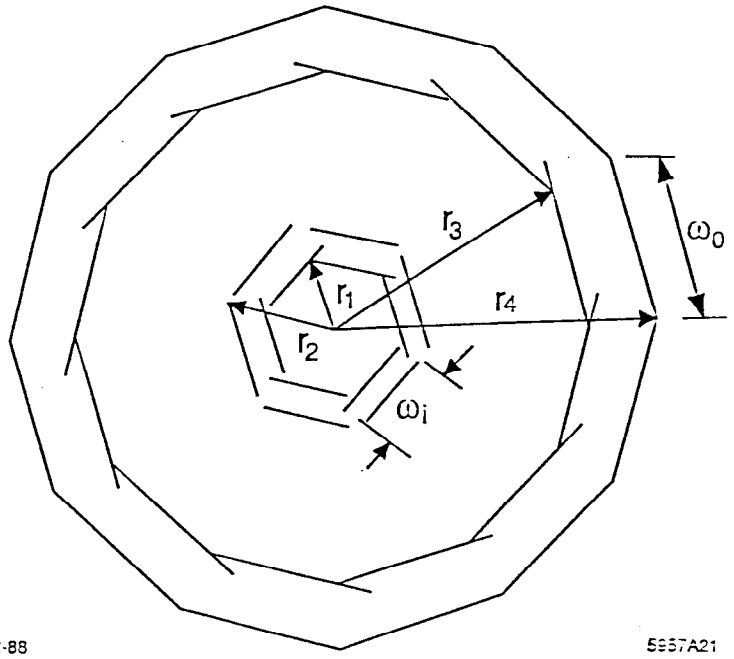


Figure 5

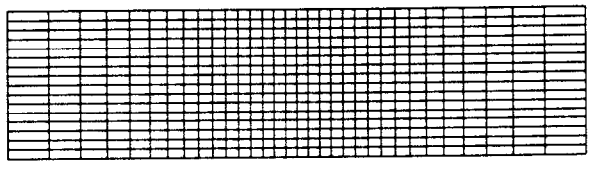

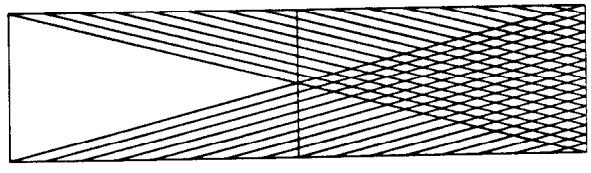

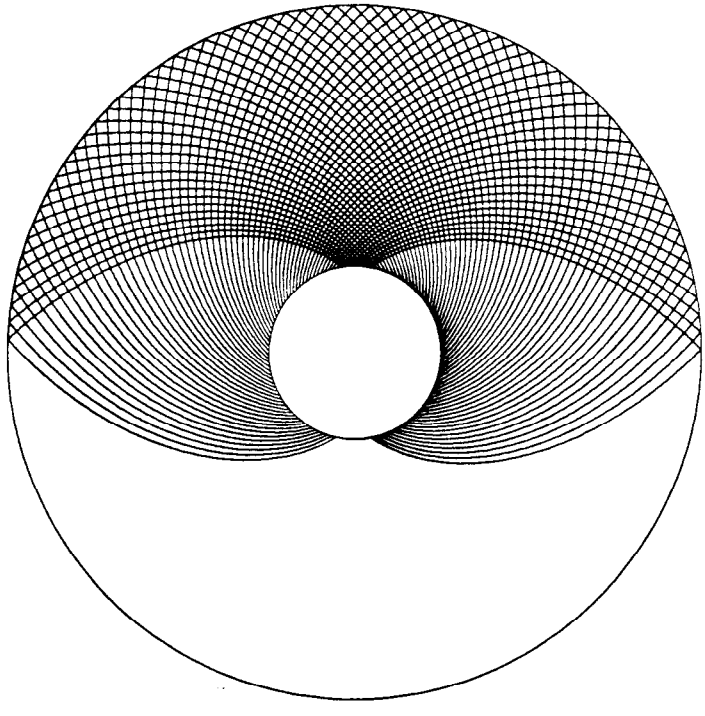

Figure 6

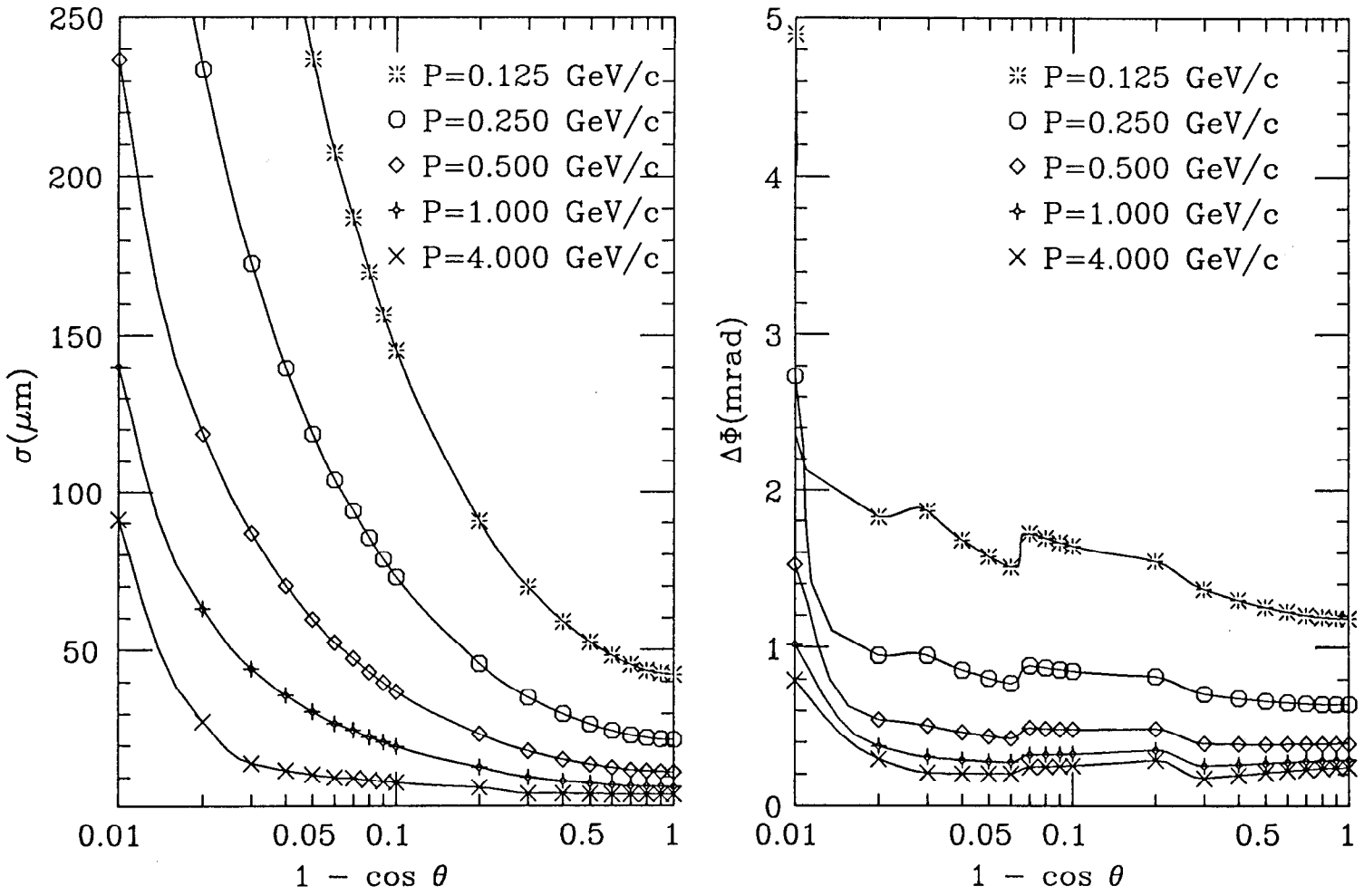
250
200
150
100
50
σ(μm)
0.01
0.05
0.1
0.5
1
1 − cos θ
P=0.125 GeV/c
P=0.250 GeV/c
P=0.500 GeV/c
P=1.000 GeV/c
P=4.000 GeV/c
5
4
3
2
1
0
ΔΦ(mrad)
0.01
0.05
0.1
0.5
1
1 − cos θ
P=0.125 GeV/c
P=0.250 GeV/c
P=0.500 GeV/c
P=1.000 GeV/c
P=4.000 GeV/c

Figure 7